Computers and Chemical Engineering 95 (2016) 38–48

Contents lists available at ScienceDirect

Computers and Chemical Engineering

journal homepage: www.elsevier.com/locate/compchemeng

An adaptive discretization MINLP algorithm for optimal synthesis of decentralized energy supply systems☆

Sebastian Goderbauer[a,b], Björn Bahl[c], Philip Voll[c], Marco E. Lübbecke[b], André Bardow[c], Arie M.C.A. Koster[a,*]

[a] Lehrstuhl II für Mathematik, RWTH Aachen University, 52056 Aachen, Germany
[b] Operations Research, RWTH Aachen University, 52072 Aachen, Germany
[c] Chair of Technical Thermodynamics, RWTH Aachen University, 52056 Aachen, Germany

ARTICLE INFO

Article history:
Received 14 June 2016
Received in revised form 6 September 2016
Accepted 8 September 2016
Available online 13 September 2016

Keywords:
Mixed-integer nonlinear programming
Decentralized energy supply system
Synthesis
Structural optimization
Adaptive discretization

ABSTRACT

Decentralized energy supply systems (DESS) are highly integrated and complex systems designed to meet time-varying energy demands, e.g., heating, cooling, and electricity. The synthesis problem of DESS addresses combining various types of energy conversion units, choosing their sizing and operations to maximize an objective function, e.g., the net present value. In practice, investment costs and part-load performances are nonlinear. Thus, this optimization problem can be modeled as a nonconvex mixed-integer nonlinear programming (MINLP) problem. We present an adaptive discretization algorithm to solve such synthesis problems containing an iterative interaction between mixed-integer linear programs (MIPs) and nonlinear programs (NLPs). The proposed algorithm outperforms state-of-the-art MINLP solvers as well as linearization approaches with regard to solution quality and computation times on a test set obtained from real industrial data, which we made available online.

1. Introduction

We propose an adaptive discretization algorithm for the superstructure-based synthesis of decentralized energy supply systems (DESS). The proposed optimization-based algorithm employs discretization of the continuous decision variables. The discretization is iteratively adapted and used to obtain valid nonconvex mixed-integer nonlinear program (MINLP) solutions within short solution time.

DESS can consist of several energy conversion components (e.g., boilers and chillers) providing different utilities (e.g., heating, cooling, electricity). DESS are highly integrated and complex systems due to the integration of different forms of energy and their connection to the gas and electricity market as well as to the energy consumers. The application of DESS encompasses, e.g., chemical parks (Maréchal and Kalitventzeff, 2003), urban districts (Maréchal et al., 2008; Jennings et al., 2014) and building complexes (Arcuri et al., 2007; Lozano et al., 2009). Energy costs usually match the companies' profits in magnitude (Drumm et al., 2013). Thus, optimally designed decentralized energy supply systems can lead to a considerable increase of profits.

The target of optimal synthesis of DESS is the identification of an (economically) optimal structure (which types of equipment and how many units?) and optimal sizing (how big?), while simultaneously considering the optimal operation of the selected components (which components are operated at which level at what time?) (Frangopoulos et al., 2002). These three decision levels could be considered sequentially. However, the levels influence each other, thus only a simultaneous optimization will find a global optimal solution. In this paper, we consider the simultaneous optimization using superstructure-based synthesis. A superstructure needs to be predefined and consists of a superset of possible components, which can be selected within the synthesis of the DESS. If the superstructure is chosen too small, optimal solutions could be excluded, if the superstructure is chosen too large, computational effort become prohibitive. Therefore some of the authors proposed a successive superstructure expansion algorithm (Voll et al., 2013b).

The synthesis of DESS contains binary decisions for the selection of energy conversion components as well as the on/off status in the operation of each component. Combined with nonlinear part-load performance of the energy conversion components, nonlinear economy-of-scale effects in the investment cost curves and strict

☆ Funded by the Excellence Initiative of the German federal and state governments.
* Corresponding author.
E-mail address: koster@math2.rwth-aachen.de (A.M.C.A. Koster).

http://dx.doi.org/10.1016/j.compchemeng.2016.09.008
0098-1354/

energy balances, the synthesis of DESS leads in general to a nonconvex MINLP (Bruno et al., 1998). Typically, an economic objective function is considered, e.g., the net present value is maximized or the total annualized costs are minimized, furthermore also ecologic objective functions can be considered (Østergaard, 2009).

Metaheuristic optimization approaches have been proposed for the synthesis of DESS: evolutionary algorithms were proposed for superstructure-free linearized synthesis as well as superstructure-based MINLP synthesis (Dimopoulos and Frangopoulos, 2008; Voll et al., 2012). Stojiljkovic et al. (2014) proposed a heuristic for structural decisions and solved an mixed-integer linear program (MILP) for operation decision. These heuristic approaches do not provide any measure of optimality.

To allow rigorous optimization, mostly linearized approaches are considered for synthesis of practically relevant problems. In the resulting MILPs, the nonlinearities are approximated by piecewise-linearized functions. First, Papoulias and Grossmann (1983) linearized the investment cost functions, the nonlinear operation conditions are modeled as discrete, but fixed operation conditions. Continuous operation decision with constant efficiency is addressed by Lozano et al. (2009) for MILP synthesis of energy supply systems in the building sector using fixed capacities. Voll et al. (2013b) proposed an MILP model accounting for piecewise-linearized part-load dependent operation conditions and piecewise-linearized investment costs for continuous component sizing. Recently, Yokoyama et al. (2015) modeled the structure decision with integer variables for the type and discrete sizes of components, thus, modeling the nonlinear investment cost curve is not required. The operation power is modeled as linear function within allowed operation ranges.

The solution of the linearization approaches only results in approximated solutions. However, solving the MINLP of superstructure-based synthesis is computationally demanding. First, an MINLP model for the operation of DESS was considered by Prokopakis and Maroulis (1996). The model takes into account the nonlinear size- and load-dependent components performance. Papalexandri et al. (1998) and Bruno et al. (1998) generalized the MINLP formulation to the optimal synthesis of DESS. Due to the complexity of the problem, only one component of each type is considered in the superstructure and the demand is considered by a single load case. An MINLP model considering multiple, detailed components as well as multiple load cases for the demand profile have been proposed by Varbanov et al. (2004, 2005). To solve the resulting large MINLP, nonlinearities of part-load performance are predefined in an iterative loop and internally MILPs are solved. Chen and Lin (2011) solved an MINLP for a steam-generation plant, the nonlinearities of part-load performance are optimized, nevertheless the model considers steam as a single demand type. The problem of integrated optimization of DESS and process system commonly results in large-scale MINLPs. Recently Zhao et al. (2015) decomposed the integrated MINLP of optimal operation of DESS and process system into an MILP and NLP problem and the variables are exchanged between both problems. Moreover, Tong et al. (2015) proposed a discretization approach for the MINLP of optimal operation of DESS and process system. Further discretization approaches for solving nonconvex MINLP problems with different practical applications are discussed in Section 3.

In this paper, MINLP solutions are obtained by an adaptive discretization algorithm for the nonlinear synthesis problem of DESS. (Commercial) MINLP solvers such as BARON (Tawarmalani and Sahinidis, 2005) reach computational limits for relative small test cases of the considered MINLP, accounting for nonlinear investment cost and multivariate nonlinear part-load dependent operation performance. We developed a problem-tailored adaptive discretization algorithm to obtain valid solutions of the MINLP within short solution time. The algorithm discretizes the continuous component size within bounds given by practically available component size limits. The whole range of size can be selected for each type of component, since the discretization is iteratively adapted. Thus, the algorithm does not require predefining discrete sizes of the components in the superstructure. Moreover, the operation of each component for each load case is discretized with finer steps depending on the part-load performance of each type of energy conversion component. Thus, various energy conversion components with different capacities and with corresponding investment and maintenance costs can be selected and adjusted to meet the energy demands in each load case.

We state our MINLP model of the DESS in Section 2. In Section 3, we describe the proposed adaptive discretization algorithm. In Section 4, we apply the algorithm to a test set of a real-world example. Solutions and performance are compared to a standard MINLP solver as well as state-of-the-art linearization approaches with MILP models.

2. Optimization models for decentralized energy supply systems

In this section, we present an MINLP model for optimal synthesis of DESS (Section 2.2) as well as a piecewise-linearized model (Section 2.3), which we use as benchmark for our adaptive discretization algorithm. First of all, in Section 2.1, notations of parameters, decisions, and the optimization problem as a whole are given.

2.1. Equipment, parameters, and decisions

The set of energy conversion units, which can be set up to meet the demands, is denoted by superstructure $S = B, \dot\cup C \dot\cup T \dot\cup A$ and encompasses a set of boilers B, a set of combined heat and power engines C, a set of turbo-driven compressor chillers T and a set of absorption chillers A (Fig. 1). Further equipment could be included, but we focus here on the problem introduced in our earlier work (Voll et al., 2013b). All units $s \in S$ in the superstructure are not further specified than their type of equipment. Note, that an optimal DESS is likely to contain multiple units of one type which is in strong contrast to classical process synthesis problems (Farkas et al., 2005).

The set of load cases considered for the operation of the DESS is denoted by L. The length of load case $\ell \in L$ is denoted by $\Delta_\ell \geq 0$. Furthermore, $\dot E_\ell^{\text{heat}} \geq 0$, $\dot E_\ell^{\text{cool}} \geq 0$, and $\dot E_\ell^{\text{el}} \geq 0$ denote the demands of heating, cooling, and electricity, which have to be satisfied with equality by the DESS in every load case $\ell \in L$. For each unit $s \in S$, its continuous size $\dot V_s^{\text{N}}$ has to be determined. The size $\dot V_s^{\text{N}}$ specifies the maximum (nominal) output energy and has to be between a minimum size $\dot V_s^{\text{N,min}}$ and a maximum size $\dot V_s^{\text{N,max}}$. For combined heat and power (CHP) engines, the output is not unique (heat and electricity). In this case, the size refers to the maximum heat output. The investment cost of unit $s \in S$ depends on its size $\dot V_s^{\text{N}}$ and is given by the nonlinear function $I_s(\dot V_s^{\text{N}})$. Further, maintenance costs are considered as constant factors m_s in terms of investment costs.

The output power of unit $s \in S$ at load case $\ell \in L$ is to be determined and is denoted by $\dot V_{s\ell}$. Again, for CHP, the output power refers to the heat output. The nonlinear function $\dot V_{s\ell}^{\text{el}}(\dot V_{s\ell}, \dot V_s^{\text{N}})$ describes the electricity output of a CHP $s \in C \subseteq S$. For each unit $s \in S$ operated in load case $\ell \in L$, a minimum part-load operation is required. Thus, the condition $\alpha_s^{\min} \dot V_s^{\text{N}} \leq \dot V_{s\ell} \leq \dot V_s^{\text{N}}$ with minimum part-load factor $0 \leq \alpha_s^{\min} \leq 1$ has to hold. If $s \in S$ is not operated in load case $\ell \in L$, we set $\dot V_{s\ell} = 0$. The input needed to generate the output $\dot V_{s\ell}$ is described by the nonlinear part-load performance function $\dot U_s(\dot V_{s\ell}, \dot V_s^{\text{N}})$.

Parameters $p^{\text{gas,buy}}$, $p^{\text{el,buy}}$, and $p^{\text{el,sell}}$ denote the purchase price of gas and electricity, and the selling price of electricity from and

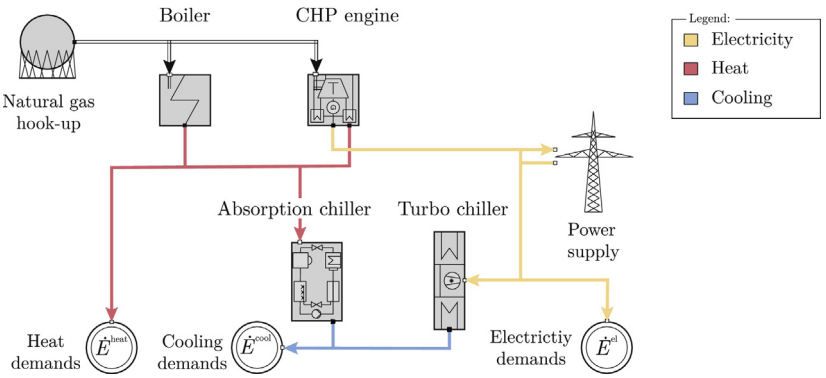

Fig. 1. Example of a decentralized energy supply system with exactly one unit of each considered type of equipment.

to the grid. To compute the objective value of a feasible DESS, i.e., the net present value, the parameter

$$\mathrm{APVF}(i, \gamma^{\mathrm{CF}}) := \frac{(i+1)^{\gamma^{\mathrm{CF}}} - 1}{i \cdot (i+1)^{\gamma^{\mathrm{CF}}}}$$

denotes the present value factor and depends on discount rate i and cash flow time γ^{CF}.

The equipment models including the analytical equations of the unit's input–output relations and all parameters can be found in Appendix A.

2.2. MINLP formulation

Variables. For every unit $s \in S$, the variable $y_s \in \{0, 1\}$ denotes whether the unit is chosen and the continuous variable $\dot{V}_s^{\mathrm{N}} \geq 0$ denotes the (nominal) size of unit s. The variable $\delta_{s\ell} \in \{0, 1\}$ denotes the on/off-status and the continuous variable $\dot{V}_{s\ell} \geq 0$ denotes the output power of unit $s \in S$ in load case $\ell \in L$. Furthermore, the continuous variables $\dot{U}_\ell^{\mathrm{el,buy}} \geq 0$ and $\dot{V}_\ell^{\mathrm{el,sell}} \geq 0$ denote the bought and sold electricity power from and to the grid in load case $\ell \in L$.

Formulation. A mixed-integer nonlinear programming formulation for the considered problem for optimal synthesis of DESS is given by (1)–(12).

$$\max \quad \mathrm{APVF}(i, \gamma^{\mathrm{CF}}) \cdot \left[\sum_{\ell \in L} \Delta_\ell \cdot \left(p^{\mathrm{el,sell}} \cdot \dot{V}_\ell^{\mathrm{el,sell}} - p^{\mathrm{el,buy}} \cdot \dot{U}_\ell^{\mathrm{el,buy}} - p^{\mathrm{gas,buy}} \cdot \sum_{s \in B \cup C} \delta_{s\ell} \cdot \dot{U}_s(\dot{V}_{s\ell}, \dot{V}_s^{\mathrm{N}}) \right) - \sum_{s \in S} m_s \cdot I_s(\dot{V}_s^{\mathrm{N}}) \cdot y_s \right] - \sum_{s \in S} I_s(\dot{V}_s^{\mathrm{N}}) \cdot y_s \tag{1}$$

$$\text{s.t.} \quad \sum_{s \in B \cup C} \dot{V}_{s\ell} = \dot{E}_\ell^{\mathrm{heat}} + \sum_{s \in A} \delta_{s\ell} \cdot \dot{U}_s(\dot{V}_{s\ell}, \dot{V}_s^{\mathrm{N}}), \quad \forall \ \ell \in L \tag{2}$$

$$\sum_{s \in A \cup T} \dot{V}_{s\ell} = \dot{E}_\ell^{\mathrm{cool}}, \quad \forall \ \ell \in L \tag{3}$$

$$\dot{U}_\ell^{\mathrm{el,buy}} + \sum_{s \in C} \delta_{s\ell} \cdot \dot{V}_s^{\mathrm{el}}(\dot{V}_{s\ell}, \dot{V}_s^{\mathrm{N}}) = \dot{E}_\ell^{\mathrm{el}} + \sum_{s \in T} \delta_{s\ell} \cdot \dot{U}_s(\dot{V}_{s\ell}, \dot{V}_s^{\mathrm{N}}) + \dot{V}_\ell^{\mathrm{el,sell}}, \quad \forall \ \ell \in L \tag{4}$$

$$\dot{V}_s^{\mathrm{N,min}} \leq \dot{V}_s^{\mathrm{N}} \leq \dot{V}_s^{\mathrm{N,max}}, \quad \forall \ s \in S \tag{5}$$

$$\dot{V}_{s\ell} \leq \delta_{s\ell} \cdot \dot{V}_s^{\mathrm{N,max}}, \quad \forall \ s \in S, \ell \in L \tag{6}$$

$$\dot{V}_{s\ell} \leq \dot{V}_s^{\mathrm{N}}, \quad \forall \ s \in S, \ell \in L \tag{7}$$

$$\dot{V}_{s\ell} \geq \alpha_s^{\min} \cdot \dot{V}_s^{\mathrm{N}} - (1 - \delta_{s\ell}) \cdot \alpha_s^{\min} \cdot \dot{V}_s^{\mathrm{N,max}}, \quad \forall \ s \in S, \ell \in L \tag{8}$$

$$y_s \geq \delta_{s\ell}, \quad \forall \ s \in S, \ell \in L \tag{9}$$

$$y_s \in \{0, 1\}, \quad \dot{V}_s^{\mathrm{N}} \geq 0, \quad \forall \ s \in S \tag{10}$$

$$\delta_{s\ell} \in \{0, 1\}, \quad \dot{V}_{s\ell} \geq 0, \quad \forall \ s \in S, \ell \in L \tag{11}$$

$$\dot{U}_\ell^{\mathrm{el,buy}}, \dot{V}_\ell^{\mathrm{el,sell}} \geq 0, \quad \forall \ \ell \in L \tag{12}$$

Objective. In objective (1), the net present value NPV : = APVF(i, γ^{CF}) · $R_{\mathrm{CF}} - I$ is maximized. The NPV is calculated from the present value factor APVF(i, γ^{CF}), the net cash flow R_{CF} and the total investments I. The net cash flow R_{CF} are the annual revenues from sold electricity $\dot{V}_\ell^{\mathrm{el,sell}}$ minus the cost for electricity $\dot{U}_\ell^{\mathrm{el,buy}}$ bought from the grid and secondary energy $\dot{U}_s(\dot{V}_{s\ell}, \dot{V}_s^{\mathrm{N}})$ consumed by the boilers and CHP engines as well as maintenance costs.

Constraints. Constraints (2)–(4) ensure that the demands for heating E_ℓ^{heat}, cooling E_ℓ^{cool} and electricity E_ℓ^{el} are fulfilled with equality in every load case $\ell \in L$ by the DESS. Constraints (5) restrict the size V_s^{N} to be in the technically allowed range $[V_s^{\mathrm{N,min}}; V_s^{\mathrm{N,max}}]$. Constraints (6)–(8) force $V_{s\ell} = 0$, if $\delta_{s\ell} = 0$ and, otherwise, limit $V_{s\ell}$ to the operation interval $[\alpha_s^{\min} \cdot V_s^{\mathrm{N}}; V_s^{\mathrm{N}}]$. Constraints (9) ensure that a unit is chosen, if it is used in at least one load case.

We note that the formulation is nonlinear due to the equipment models of the units (Appendix A) and bilinear terms in (1), (2) and (4) as well as nonconvex due to the investment cost function $I_s(\dot{V}_s^{\mathrm{N}})$ (Appendix A) and nonlinear equality constraints (2) and (4).

2.3. Benchmarking to piecewise-linearized approach

The MINLP synthesis model (1)–(12) is commonly linearized for practical applications (Section 1). The solution obtained by the approximated MILP is in general not feasible for the nonlinear model (Bruno et al., 1998) (Section 4.2). In this section, we present an approach to obtain feasible solutions of the MINLP based on solutions of the MILP. The feasible MINLP solution based on the MILP result is considered as benchmark for our adaptive discretization algorithm (Section 3). Since, as explained above, a one-to-one comparison between MINLP and MILP solutions is not possible, we think that the presented analysis provides an insightful comparison between previous work and the algorithm proposed in this work.

The MILP stated by Voll et al. (2013b) with piecewise-linearized functions for the nonlinear investment cost curves and piecewise-linearized part-load operation curves are employed to compute the MILP solution. To obtain a feasible MINLP solution based on

the solution $\delta^*_{s\ell}, \dot{V}^*_{s\ell}, y^*_s, \dot{V}^{N*}_s$ of the MILP, we solve MINLP$^{\text{lin,feas}}$ (13)–(15).

$$\min \quad |L| \cdot \sum_{s \in S} \left(\frac{\left| \dot{V}^{N*}_s - \dot{V}^{N}_s \right|}{\dot{V}^{N*}_s} \right) + \sum_{\substack{s \in S, \ell \in L: \\ \delta^*_{s\ell} = 1}} \left(\frac{\left| \dot{V}^*_{s\ell} - \dot{V}_{s\ell} \right|}{\dot{V}^*_{s\ell}} \right) \quad (13)$$

$$\text{s.t.} \quad (2) - (12) \quad (14)$$

$$y_s = y^*_s, \quad \delta_{s\ell} = \delta^*_{s\ell}, \quad \forall s \in S, \ell \in L \quad (15)$$

The selected structure of the DESS y^*_s and the on/off status of the equipment $\delta^*_{s\ell}$ defined by the MILP is kept fixed. The objective function reflects minimizing the difference between the solution values of the MILP and the MINLP, in the solution space of the MINLP. Thus, feasible solutions for the MINLP are obtained which are 'near' the given solution of the MILP. The difference measure is defined by the sum of the normalized differences in optimal design $\dot{V}^N_s$ and operation $\dot{V}_{s\ell}$.

3. Adaptive discretization algorithm

Solving the nonconvex MINLP (1)–(12) with state-of-the-art solvers like BARON (Tawarmalani and Sahinidis, 2005) leads to unsatisfying results. For several nontrivial test instances, it is even hard for solvers to compute a feasible solution (Section 4). Thus, the need of a problem-specific solution method providing primal MINLP solutions is evident.

It is a common approach to discretize (continuous) variables in a nonconvex nonlinear program to approximate it with an easier to solve mixed-integer linear one (e.g., Leyffer et al., 2008; Pham et al., 2009; Geißler et al., 2011; Gupte et al., 2013; Kolodziej et al., 2013; Yue and You, 2014). As an obtained solution might not be feasible for the original MINLP, we extend the discretization approach. Given an approximate solution, we fix selected solution-specific decisions (i.e., unit sizes and on/off statuses in the load cases), and solve the remaining NLP using a decomposition to arrive at a primal MINLP solution. To have a computational tractable approximation, only a few discretization points for the unit size and operation are used. However, to ensure a certain accuracy in our discretization algorithm, this two step algorithm is embedded in a loop of refinements of the discretization. At every iteration, the discretization grid is contracted and shifted in the direction of the discrete unit size chosen in the previous iteration, keeping the size of the discretized MILP.

The discretized problem formulation of the nonconvex MINLP (1)–(12) is described in Section 3.1, followed by the procedure to form a feasible MINLP solution using the approximate solution in Section 3.2. The adaptive part of the discretization algorithm is specified in Section 3.3. In the end and putting everything together, Section 3.4 provides a description of the adaptive discretization algorithm as a whole and some further comments.

3.1. Discretized problem

To develop an approximation via discretization, we discretize all continuous variables with nonlinear dependencies. In MINLP (1)–(12) this involves the unit's size $\dot{V}^N_s \geq 0$ and operation $\dot{V}_{s\ell} \geq 0$.

Unit size. If unit $s \in S$ is chosen, i.e., $y_s = 1$ holds, we have to choose a size $\dot{V}^N_s$ in the interval $[\dot{V}^{N,\min}_s, \dot{V}^{N,\max}_s]$. The investment cost function $I_s(\dot{V}^N_s)$ depends on the unit's size and is nonlinear (Appendix A). We discretize the range of the continuous variable $\dot{V}^N_s \in [\dot{V}^{N,\min}_s, \dot{V}^{N,\max}_s]$ by dividing the interval into $k^{\max}_s$ (equidistant) discrete sizes

$$\dot{V}^{N,\text{val}}_{s1} < \dot{V}^{N,\text{val}}_{s2} < \ldots < \dot{V}^{N,\text{val}}_{sk^{\max}_s}$$

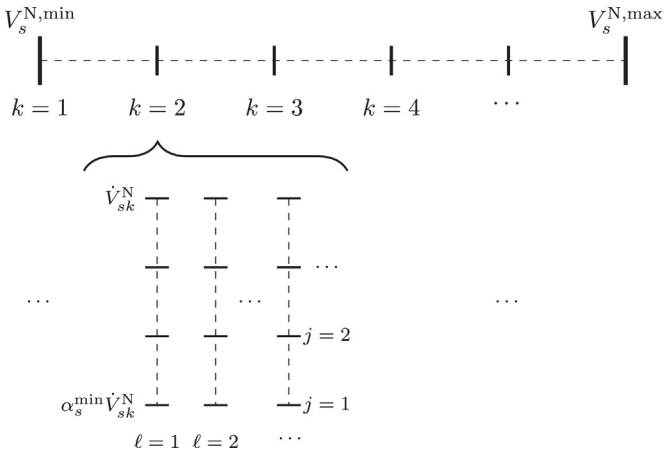

Fig. 2. Discretization and notation of unit size decisions (top) and operation decisions (bottom).

with $\dot{V}^{N,\min}_s \leq \dot{V}^{N,\text{val}}_{s1}, \dot{V}^{N,\text{val}}_{sk^{\max}_s} \leq \dot{V}^{N,\max}_s$ and $k^{\max}_s \in \mathbb{N}$ an odd number. These $\dot{V}^{N,\text{val}}_{sk}$ are parameters and the related variables $\dot{V}^N_{sk} \in \{0,1\}$ denote whether unit $s \in S$ is set up with the kth discrete size $\dot{V}^{N,\text{val}}_{sk}$. Thus, we transform every continuous variable $\dot{V}^N_s$ in several binary variables $\dot{V}^N_{sk}$. This implies that we do not need the nonlinear investment cost function in the discretized problem anymore, because for each discrete size $\dot{V}^{N,\text{val}}_{sk}$ we can compute its investment costs $I^{\text{val}}_{sk} := I_s(\dot{V}^{N,\text{val}}_{sk})$ in advance.

Unit operation. Together with the unit's size, one can compute the input energy needed to get a desired operation output $\dot{V}_{s\ell}$ using the nonlinear part-load performance functions $\dot{U}_s(\dot{V}_{s\ell}, \dot{V}^N_s)$ (Appendix A). If $\dot{V}^{N,\text{val}}_{sk}$ is chosen out of the discrete unit sizes and the unit is switched on, the possible output $\dot{V}_{s\ell}$ of this unit is bound by the size $\dot{V}^{N,\text{val}}_{sk}$ and a minimal possible part-load $\alpha^{\min}_s \dot{V}^{N,\text{val}}_{sk}$ with $0 \leq \alpha^{\min}_s \leq 1$. Again, we discretize the range of the continuous variable $\dot{V}_{s\ell} \in [\alpha^{\min}_s \dot{V}^{N,\text{val}}_{sk}, \dot{V}^{N,\text{val}}_{sk}]$ by dividing the interval into $j^{\max}_{sk\ell}$ (equidistant) discrete operations

$$\alpha_s \cdot \dot{V}^{N,\text{val}}_{sk} =: \dot{V}^{\text{val}}_{sk\ell 1} < \dot{V}^{\text{val}}_{sk\ell 2} < \ldots < \dot{V}^{\text{val}}_{sk\ell j^{\max}_{sk\ell}} := \dot{V}^{N,\text{val}}_{sk}$$

with $j^{\max}_{sk\ell} \in \mathbb{N}$ and $j^{\max}_{sk\ell} \geq 2$. The variable $\dot{V}_{sk\ell j} \in \{0,1\}$ denotes whether unit $s \in S$ with size $\dot{V}^{N,\text{val}}_{sk}$ has the jth discrete operational output $\dot{V}^{\text{val}}_{sk\ell j}$ in load case $\ell \in L$. We name

$$\dot{U}^{\text{val}}_{sk\ell j} := \dot{U}_s(\dot{V}^{\text{val}}_{sk\ell j}, \dot{V}^{N,\text{val}}_{sk}) \quad \text{and} \quad \dot{V}^{\text{el,val}}_{sk\ell j} := V^{\text{el}}_s(\dot{V}^{\text{val}}_{sk\ell j}, \dot{V}^{N,\text{val}}_{sk})$$

the values of the employed part-load performance function at the corresponding discrete size and discrete operation.

The discretization grid of size and operation and its notation is summarized in Fig. 2.

Since fulfilling the energy demands in heating, cooling, and electricity with equality is a requirement of our problem (constraints (2)–(4)), we want to enable equality in the energy balances of our discretized approximation as well (cf. Remark 1 in Section 3.4). A pure discretization with binary variables $\dot{V}_{sk\ell j}$ does not allow this in general. Therefore, we piecewise linearize the part-load performance functions $\dot{U}_s$ and $\dot{V}^{\text{el}}_s$ using $\dot{V}^{\text{val}}_{sk\ell j}$ as supporting points. We introducing a continuous variable

$$\dot{V}^{\text{cont}}_{sk\ell j} \geq 0 \quad \text{with} \quad \dot{V}^{\text{cont}}_{sk\ell j} \leq \dot{V}^{\text{val}}_{sk\ell j+1} - \dot{V}^{\text{val}}_{sk\ell j} =: \dot{V}^{\text{val,diff}}_{sk\ell j}$$

and parameters

$$\dot{U}^{\text{lin}}_{sk\ell j} := \frac{\dot{U}^{\text{val}}_{sk\ell j+1} - \dot{U}^{\text{val}}_{sk\ell j}}{\dot{V}^{\text{val,diff}}_{sk\ell j}}, \quad \dot{V}^{\text{el,lin}}_{sk\ell j} := \frac{\dot{V}^{\text{el,val}}_{sk\ell j+1} - \dot{V}^{\text{el,val}}_{sk\ell j}}{\dot{V}^{\text{val,diff}}_{sk\ell j}}$$

for each simplex, i.e., line segment between $\dot{V}^{\text{val}}_{sk\ell j}$ and $\dot{V}^{\text{val}}_{sk\ell j+1}$. Note that in the proposed approach the discretization of the unit *size* remains a pure one, where we do not add further continuous variables or piecewise linearize anything there.

Using the specified discretization and linearization, we are able to approximate the original MINLP (1)–(12) with the following mixed-integer linear program (16)–(26) (discretized MIP). For better readability, the limits of the indices $k = 1, 2, \ldots, k^{\max}_s$ and $j = 1, 2, \ldots, j^{\max}_{sk\ell}$ are not mentioned explicitly in the following formulation and sections. Indices s and ℓ without any set information mean $s \in S$ and $\ell \in L$.

$$\begin{aligned}\max \quad & \text{APVF}(i, \gamma^{\text{CF}}) \cdot \Bigg[\sum_{\ell \in L} \Delta_\ell \cdot \Big(p^{\text{el,sell}} \cdot \dot{V}^{\text{el,sell}}_\ell - p^{\text{el,buy}} \cdot \dot{U}^{\text{el,buy}}_\ell \\ & - p^{\text{gas,buy}} \cdot \sum_{s \in B \cup C} \sum_{k,j} (\dot{U}^{\text{val}}_{sk\ell j} \cdot \dot{V}_{sk\ell j} + \dot{U}^{\text{lin}}_{sk\ell j} \cdot \dot{V}^{\text{cont}}_{sk\ell j}) \Big) \\ & - \sum_{s,k} m_s \cdot I^{\text{val}}_{sk} \cdot \dot{V}^{\text{N}}_{sk} \Bigg] - \sum_{s,k} I^{\text{val}}_{sk} \cdot \dot{V}^{\text{N}}_{sk} \end{aligned} \tag{16}$$

$$\begin{aligned}\text{s.t.} \quad & \sum_{s \in B \cup C} \sum_{k,j} (\dot{V}^{\text{val}}_{sk\ell j} \cdot \dot{V}_{sk\ell j} + \dot{V}^{\text{cont}}_{sk\ell j}) = \dot{E}^{\text{heat}}_\ell + \sum_{s \in A} \sum_{k,j} (\dot{U}^{\text{val}}_{sk\ell j} \cdot \dot{V}_{sk\ell j} \\ & + \dot{U}^{\text{lin}}_{sk\ell l} \cdot \dot{V}^{\text{cont}}_{sk\ell j}), \quad \forall \ \ell \in L \end{aligned} \tag{17}$$

$$\sum_{s \in A \cup T} \sum_{k,l} (\dot{V}^{\text{val}}_{sk\ell j} \cdot \dot{V}_{sk\ell j} + \dot{V}^{\text{cont}}_{sk\ell j}) = \dot{E}^{\text{cool}}_\ell, \quad \forall \ \ell \in L \tag{18}$$

$$\begin{aligned} & \dot{U}^{\text{el,buy}}_\ell + \sum_{s \in C} \sum_{k,j} (\dot{V}^{\text{el,val}}_{sk\ell j} \cdot \dot{V}_{sk\ell j} + \dot{V}^{\text{el,lin}}_{sk\ell j} \cdot \dot{V}^{\text{cont}}_{sk\ell j}) = \dot{E}^{\text{el}}_\ell + \dot{V}^{\text{el,sell}}_t \\ & + \sum_{s \in T} \sum_{k,j} (\dot{U}^{\text{val}}_{sk\ell j} \cdot \dot{V}_{sk\ell j} + \dot{U}^{\text{lin}}_{sk\ell j} \cdot \dot{V}^{\text{cont}}_{sk\ell j}), \quad \forall \ \ell \in L \end{aligned} \tag{19}$$

$$\dot{V}^{\text{cont}}_{sk\ell j} \le \dot{V}^{\text{val,diff}}_{sk\ell j} \cdot \dot{V}_{sk\ell j}, \quad \forall \ s, k, \ell, j \tag{20}$$

$$\sum_k \dot{V}^{\text{N}}_{sk} \le 1, \quad \forall \ s \in S \tag{21}$$

$$\sum_j \dot{V}_{sk\ell j} \le \dot{V}^{\text{N}}_{sk}, \quad \forall \ s, k, \ell \tag{22}$$

$$\dot{V}^{\text{N}}_{sk} \in \{0, 1\}, \quad \forall \ s, k \tag{23}$$

$$\dot{V}_{sk\ell j} \in \{0, 1\}, \quad \forall \ s, k, \ell, j \tag{24}$$

$$\dot{V}^{\text{cont}}_{sk\ell j} \ge 0, \quad \forall \ s, k, \ell, j \tag{25}$$

$$\dot{U}^{\text{el,buy}}_\ell, \dot{V}^{\text{el,sell}}_\ell \ge 0, \quad \forall \ \ell \in L \tag{26}$$

The binary variables y_s and $\delta_{s\ell}$ in MINLP formulation (1)–(12) are not needed anymore, since the new binary variables $\dot{V}^{\text{N}}_{sk}$ and $\dot{V}_{sk\ell j}$ together with constraints (21) and (22) include their role. Of course, the discretized problem (16)–(26) contains a lot more binary decisions, but the nonlinearities and actually the nonconvex nonlinearities are eliminated in that model. The discretized problem (16)–(26) is a mixed-integer linear program. Moreover, some binary variables $\dot{V}^{\text{N}}_{sk}$ and $\dot{V}_{sk\ell j}$ can be eliminated by preprocessing (Section 4.2) depending on the demands.

3.2. Nonlinear feasibility

After computing a solution of (16)–(26), post processing is needed to compute a primal feasible solution of the original MINLP (1)–(12). For this post processing, we fix the unit sizes and load case specific on/off statuses given by the approximate solution. Therefore, let $\dot{V}^{\text{N}*}_{sk} \in \{0, 1\}$ and $\dot{V}^{*}_{sk\ell j} \in \{0, 1\}$ be the values of the related variables of a given discretized problem solution. For each unit $s \in S$ and load case $\ell \in L$ parameters

$$y^{\text{par}}_s := \sum_k \dot{V}^{\text{N}*}_{sk} \tag{27}$$

$$\dot{V}^{\text{N,par}}_s := \sum_k \dot{V}^{\text{N,val}}_{sk} \cdot \dot{V}^{\text{N}*}_{sk} \tag{28}$$

$$\delta^{\text{par}}_{s\ell} := \sum_{k,j} \dot{V}^{*}_{sk\ell j} \tag{29}$$

are defined. Fixing the variables $y_s \in \{0, 1\}$, $\dot{V}^{\text{N}}_s \ge 0$ and $\delta_{s\ell} \in \{0, 1\}$ with these values in MINLP (1)–(12) implies that all binary variables and all constraints (5)–(9) linking load case are not needed anymore or become variables bounds. As a consequence, the problem is decomposable in independent nonlinear programs, one for every load case $\ell \in L$, named NLP_ℓ. Since the equality constraints (2) and (4) are still present, every NLP_ℓ remains nonconvex. However, as the computational results show in Section 4, the independent problems are solved quite fast for the considered test instances. It is not guaranteed that NLP_ℓ provides a feasible solution, since parts of an approximate solution are fixed. Whether NLP_ℓ provides a feasible solution depends on the form of the piecewise linearized functions and on the fineness of the discretization. It turns out that more discretization points, on the one hand, enlarge the probability to determine a feasible solution in NLP_l but, on the other hand, enlarge the computation times of solving NLP_l. However, the computational results (Section 4.2) show that for all test instances considered in this paper every single NLP_ℓ was feasible.

3.3. Adapting discretization

Solving the discretized problem (16)–(26) followed by suited NLPs for nonlinear feasibility, a primal solution of the MINLP (1)–(12) is probably computed. This interaction of MIP and NLPs is incorporated into an iteration loop, as it is described as a whole in Section 3.4. At the end of every iteration step, the discretization grid is adapted based on the just computed solution of the discretized problem in that step. Thereby, nearly the entire spectrum of possible unit sizes is enabled and a greater accuracy in the whole algorithm and therefore better primal solutions are achieved. In the rest of this section, the procedure of adapting the discretization is described in detail. Proceed to Section 3.4 for an overview of the whole adaptive discretization algorithm.

Let $\dot{V}^{\text{N,val}}_{s1} < \dot{V}^{\text{N,val}}_{s2} < \ldots < \dot{V}^{\text{N,val}}_{sk^{\max}_s}$ be the discretization of the size of unit $s \in S$ in a certain iteration step and let $1 \le k^*_s \le k^{\max}_s$ be the index of the chosen discrete size of unit $s \in S$, i.e., $\dot{V}^{\text{N,par}}_s = \dot{V}^{\text{N,val}}_{sk^*_s}$ holds (cf. Eq. (28)). We are faced with three different cases depending on k^*_s and $\dot{V}^{\text{N,par}}_s$:

Case 1 (interior point): $k^*_s \notin \{1, k^{\max}_s\}$

Case 2 (interval limit): $k^*_s \in \{1, k^{\max}_s\}$ and $\dot{V}^{\text{N,val}}_{sk^*_s} \notin \{\dot{V}^{\text{N,min}}_s, \dot{V}^{\text{N,max}}_s\}$

Case 3 (bound): $k^*_s \in \{1, k^{\max}_s\}$ and $\dot{V}^{\text{N,val}}_{sk^*_s} \in \{\dot{V}^{\text{N,min}}_s, \dot{V}^{\text{N,max}}_s\}$

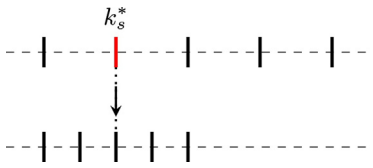

Fig. 3. Adaptive discretization (interior point).

Case 1 (interior point). For the case $k_s^* \notin \{1, k_s^{\max}\}$ the chosen discrete point lies not at the end of the discretization interval. We then contract the discrete grid points in the direction of the chosen size $\dot{V}_{sk_s^*}^{\mathrm{N,val}}$. More precisely, the equidistant division of the interval $[V_{sk_s^*-1}^{\mathrm{N,val}}, V_{sk_s^*+1}^{\mathrm{N,val}}]$ gets the new and adapted discretization. Notice, since $k_s^{\max}$ is odd, $\dot{V}_s^{\mathrm{N,par}}$ stays to be a grid point after the adaption (Fig. 3).

Example (interior point). For $k_s^{\max} = 5$, $k_s^* \notin \{1, 5\}$ the adaption effects:

$$\begin{aligned}
\dot{V}_{s1}^{\mathrm{N,val}} &\leftarrow V_{sk_s^*-1}^{\mathrm{N,val}} \\
\dot{V}_{s2}^{\mathrm{N,val}} &\leftarrow \frac{1}{2}\left(V_{sk_s^*}^{\mathrm{N,val}} + V_{sk_s^*-1}^{\mathrm{N,val}}\right) \\
\dot{V}_{s3}^{\mathrm{N,val}} &\leftarrow V_{sk_s^*}^{\mathrm{N,val}} \\
\dot{V}_{s4}^{\mathrm{N,val}} &\leftarrow \frac{1}{2}\left(V_{sk_s^*+1}^{\mathrm{N,val}} + V_{sk_s^*}^{\mathrm{N,val}}\right) \\
\dot{V}_{s5}^{\mathrm{N,val}} &\leftarrow V_{sk_s^*+1}^{\mathrm{N,val}}.
\end{aligned}$$

Case 2 (interval limit). If $k_s^* \in \{1, k_s^{\max}\}$ is the index of one of the end points of the discretization and $\dot{V}_{sk_s^*}^{\mathrm{N,val}} \notin \{\dot{V}_s^{\mathrm{N,min}}, \dot{V}_s^{\mathrm{N,max}}\}$ holds, we shift the grid in the direction of the chosen size (and do not contract it). Thus, for $k_s^* = 1$ (case $k_s^* = k_n^{\max}$ analog) the equidistant division of the interval

$$\left[2 \cdot \dot{V}_{sk_s^*}^{\mathrm{N,val}} - \dot{V}_{s\lceil \frac{k_s^{\max}}{2} \rceil}^{\mathrm{N,val}}, \dot{V}_{s\lceil \frac{k_s^{\max}}{2} \rceil}^{\mathrm{N,val}}\right]$$

results in the adapted discretization (Fig. 4a). It is guaranteed that this discretization respects the initial size bounds $\dot{V}_s^{\mathrm{N,min}}$ and $\dot{V}_s^{\mathrm{N,max}}$.

Case 3 (bound). In the remaining case of $k_s^* \in \{1, k_s^{\max}\}$ and $\dot{V}_{sk_s^*}^{\mathrm{N,val}} \in \{\dot{V}_s^{\mathrm{N,min}}, \dot{V}_s^{\mathrm{N,max}}\}$ the chosen discrete point lies at a bound. Here, we assume $k_s^* = 1$ and $\dot{V}_{sk_s^*}^{\mathrm{N,val}} = \dot{V}_s^{\mathrm{N,min}}$ (other case analog). We contract the discretization, respecting the bounds $\dot{V}_s^{\mathrm{N,min}}$ and $\dot{V}_s^{\mathrm{N,max}}$. The equidistant division of the interval $[\dot{V}_s^{\mathrm{N,min}}, \dot{V}_{s\lceil \frac{k_s^{\max}}{2} \rceil}^{\mathrm{N,val}}]$ is the adapted discretization (Fig. 4b).

Example (interval limit, bound). Fig. 4 shows examples for the adaption of the discretization in case 2 and 3.

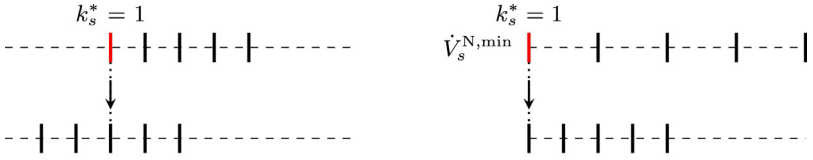

(a) case 2: chosen (interval limit) (b) case 3 (bound)

Fig. 4. Adaptive discretization: (a) case 2 and (b) case 3.

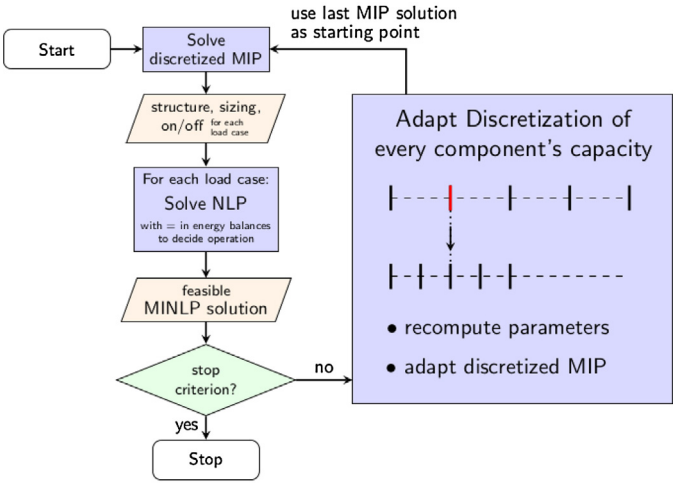

Fig. 5. Adaptive discretization algorithm.

3.4. Adaptive discretization algorithm

The adaptive discretization algorithm is shown in Fig. 5 as a whole. The algorithm consists of an iteration loop with a certain stop criterion, for example concerning an iteration or convergence limit. If the criterion is fulfilled, the algorithm terminates and the best MINLP solution found is the output of the algorithm, otherwise, the algorithm continues with the next iteration step. Each step consists of (i) solving the discretized problem (Section 3.1) and (ii) solving NLP_ℓ for all $\ell \in L$ with parameters and bounds computed by (27)–(29) to obtain a primal MINLP solution for the original problem (Section 3.2). After that and in the case of nontermination, (iii) the discretization is adapted as it is described in Section 3.3. All parameters concerning the discretization grid, including the operation discretizations $\dot{V}_{sk\ell 1}^{\mathrm{val}} < \dot{V}_{sk\ell 2}^{\mathrm{val}} < \ldots < \dot{V}_{sk\ell j_{sk\ell}^{\max}}^{\mathrm{val}}$, which are based on the discrete sizes, and the formulation of the discretized problem (16)–(26) are updated. The next iteration step of the algorithm starts with solving the adapted discretized problem. Notice that the last iteration's solution of the discretized problem can be used to warm-start the discretized MIP, since the discrete decisions are still feasible in the adapted grid. This improves the performance of solving the MIP.

Remark 1. *Alternative approximations for the discretized problem.* To enable equality in the energy balances in the discretized problem, we expand the pure discretization of the operation to a piecewise linearization (Section 3.1). However, this is not necessary for the functionality of the proposed algorithm, since the discretized MIP is only used as an approximation of the original problem. We developed and tested other approaches for approximating the problem via discretization in addition to the discretized MIP (16)–(26). In a pure discretization, without the piecewise linearization, we can only request for at least fulfilling the energy demands. Consequently, energy excesses are possible. These excesses can occur since it is more favorable to produce

electricity using CHP engines than to purchase it from the power grid. Thus, additional heat production by CHP engines can decrease operational costs of DESS. For that reason, there is more energy excess in solutions of a pure discretization than might be expected. Consequently, the approximation quality gets worse since overproduction is not allowed in the original problem. We develop two approaches to restrict the amount of energy excess in the pure discretization and to improve the approximation quality: First, by adding new and nontrivial constraints to the discretized problem, secondly, by penalizing energy excess in the objective function. It turns out that our adaptive discretization algorithm using the discretized problem with piecewise linearization of Section 3.1 outperforms these more sophisticated alternatives on the set of test instances (Section 4.1).

4. Computational study and results

In the computational study, we analyze the solution quality of our adaptive discretization algorithm (short AdaptDiscAlgo, Section 3) in comparison to (i) primal solutions of MINLP (Section 2.2) computed with BARON and to (ii) approximate solutions of piecewise linearized models following the explanations in Section 2.3. Furthermore, we examine the running times of all solving approaches.

Section 4.1 gives an overview and references of the online available considered test instances and Section 4.2 contains some details on the implementation of all approaches for computing MINLP solutions to synthesis of DESS. The computational results are presented in Section 4.3.

4.1. Problem instances

For the computational study on the performance our algorithm, we derived a test-set: DESSLib (Bahl et al., 2016). The DESSLib contains categorized problem instances based on the original real-world example stated by Voll et al. (2013b). The categories are characterized by 2 dimensions, the number of considered units in the superstructure and the number of considered load cases. The category for the number of considered units is denoted by *S*4, *S*8, *S*12, *S*16, e.g., *S*4 corresponds to one unit for each type of equipment. The number of considered load cases is denoted by *L*1, *L*2, *L*4, *L*6, *L*8, *L*12, *L*16, *L*24. Each category (e.g., *S*8*L*4) consists of 10 instances with stochastic variations around the original demand time-series. We assigned stochastic variations with Latin hypercube sampling (Iman et al., 1981) and a variation of ±5% of the original demand. Thus, the resulting DESSLib consists of 320 problem instances. We use the DESSLib to evaluate the performance of the proposed adaptive discretization algorithm. The short notation, e.g., *S*4*L*{1, 2} denotes the set of all test instances of categories *S*4*L*1 and *S*4*L*2.

4.2. Implementation

Software and machine. Our adaptive discretization algorithm (Section 3) was implemented in GAMS 24.4.3 (GAMS Development Corporation, 2015) using its Python-API. Computations are performed on one core of a Linux maschine with 3.40 GHz Intel Core i7-3770 processor and 32 GB RAM. To solve mixed-integer linear programs, i.e., discretized MIP (16)–(26) and MILP by Voll et al. (2013b) (Section 2.3), we use the default setting of CPLEX 12.6.1.0 (IBM, 2015). To solve (mixed-integer) nonlinear programs, i.e., MINLP (1)–(12), feasibility NLP (Section 3.2) and MINLP$^{\text{lin,feas}}$ (13)–(15), we use the default setting of BARON 14.4.0 (Tawarmalani and Sahinidis, 2005). BARON was selected as MINLP solver due its robustness in a preliminary study.

Table 1
DESS structure and equipment sizes computed by solution approaches MINLP, MINLP$^{\text{lin,feas}}$, and AdaptDiscAlgo for DESSLib's instance S8L4_8.

	MINLP	MINLP$^{\text{lin,feas}}$	AdaptDiscAlgo
Boiler #1	12.02 MW	11.45 MW	10.53 MW
Boiler #2	–	–	0.10 MW
CHP engine #1	3.20 MW	2.50 MW	3.20 MW
CHP engine #2	2.35 MW	2.30 MW	2.15 MW
Turbo chiller #1	7.88 MW	3.17 MW	3.48 MW
Turbo chiller #2	–	1.88 MW	1.90 MW
Absorption chiller #1	6.05 MW	6.43 MW	6.50 MW
Absorption chiller #2	–	2.43 MW	2.07 MW
Net present value	$-6.81 \cdot 10^7$	$-5.00 \cdot 10^7$	$-4.85 \cdot 10^7$

Discretization grid. The number of discrete sizes $k_s^{\max}$ and the number of discrete operations $j_{sk\ell}^{\max}$ in the discretized problem (Section 3.1) are $k_s^{\max} = 5$ and, with some exceptions, $j_{sk\ell}^{\max} = 10$. However, if the interval of possible operations $[\alpha_s^{\min}\dot{V}_{sk}^{\mathrm{N,val}}, \dot{V}_{sk}^{\mathrm{N,val}}]$ is smaller than 1800 kW, we reduce $j_{sk\ell}^{\max} \leq 10$ as much as necessary so that $\dot{V}_{sk\ell j}^{\mathrm{val,diff}} \geq 200$ kW or $j_{sk\ell}^{\max} = 2$ holds. These parameters have been determined in preliminary studies.

Limits and stop criterion. For solving the discretized MIP (Section 3.1), a time limit of 300 seconds is implemented in the very first iteration step of an algorithm run. For any further step, this time limit is set to 100 seconds and the last iteration's solution is used as a starting point. The time limit for solving the feasibility NLP (Section 3.2) is set to 100 seconds. Limits for the optimality gap are 0.1% (discretized MIP) and 0.001% (feasibility NLP). The adaptive discretization algorithm terminates, if the running time reaches the limit of one hour or the improvement of the best MINLP solution is less than 0.1% over the last two iteration steps.

For the benchmark MINLP (1)–(12), the same limit of one hour running time is implemented in each case. To obtain a feasible MINLP solution based on an approximate MILP solution, we solve MILP by Voll et al. (2013b) (Section 2.3) with a time limit of one hour and thereafter we solve MINLP$^{\text{lin,feas}}$ (13)–(15) with a time limit of one hour as well.

Preprocessing on discretization grid. Depending on the input data, particularly the demands of the load cases, some binary variables $\dot{V}_{sk}^{\mathrm{N}}$, $\dot{V}_{sk\ell j}$ can be eliminated by preprocessing. For chiller units $s \in A \cup T$, the operation variables $\dot{V}_{sk\ell j} \in \{0, 1\}$ with $\dot{V}_{sk\ell j}^{\mathrm{val}} > \dot{E}_{\ell}^{\mathrm{cool}}$, i.e., supply greater than demand, will not be part of any feasible solution of the discretized problem. In analogy, for heat-producing units $s \in B \cup C$, an upper bound for $\dot{V}_{sk\ell j}^{\mathrm{val}}$ is given by the heat demand $\dot{E}_{\ell}^{\mathrm{heat}}$ plus the maximal possible heat demand of absorption chillers $s \in A$. If for indices s, k these constraints remove all discrete operation variables $\dot{V}_{sk\ell j}$, the corresponding discrete size variable $\dot{V}_{sk}^{\mathrm{N}}$ can be eliminated as well. This preprocessing on the discretization grid is quite natural, however, its effect may not be underestimated, because of the large number of binary variables in the discretized problem.

4.3. Computational results

Before we analyze the robustness of our proposed algorithm compared to the two benchmarking approaches on basis of the entire set of 320 instances, we focus on one randomly chosen instance and compare the numerical solution results, i.e., DESS structure and equipment sizes, of all three considered approaches. Table 1 shows the DESS structure and equipment sizes (numbers rounded) for DESSLib's instance S8L4_8 obtained by the solution approaches MINLP (Section 2.2), MINLP$^{\text{lin,feas}}$ (Section 2.3), and AdaptDiscAlgo (Section 3). Table 1 does not contain the DESS resulting from the MILP of Voll et al. (2013b), which was the basis for the MINLP$^{\text{lin,feas}}$ solution (cf. Section 2.3). The MILP solution differs from the MINLP$^{\text{lin,feas}}$ solution just in a small increase of the boiler's

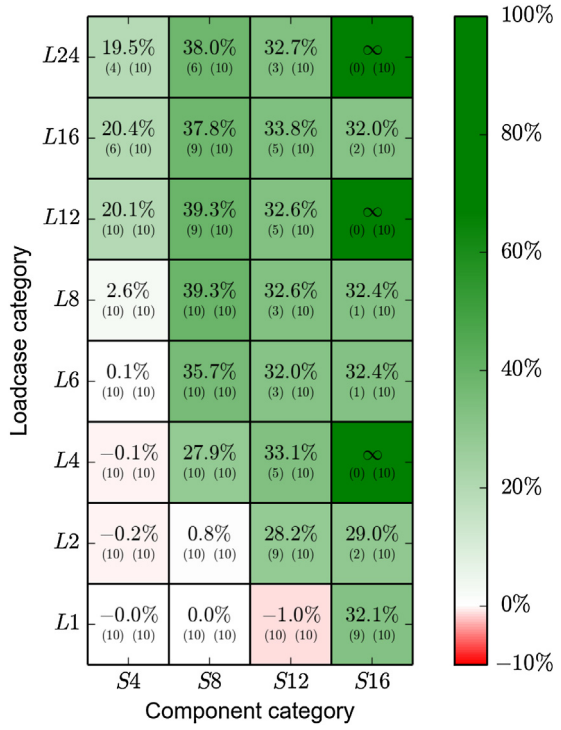

Fig. 6. Heatmap on the improvement of solution quality of AdaptDiscAlgo in relation to MINLP (1)–(12); averaged for each test instance category. In brackets: number of test instances (max. 10 per category), for which MINLP (left) respectively AdaptDiscAlgo (right) computes at least one MINLP solution in the time limit.

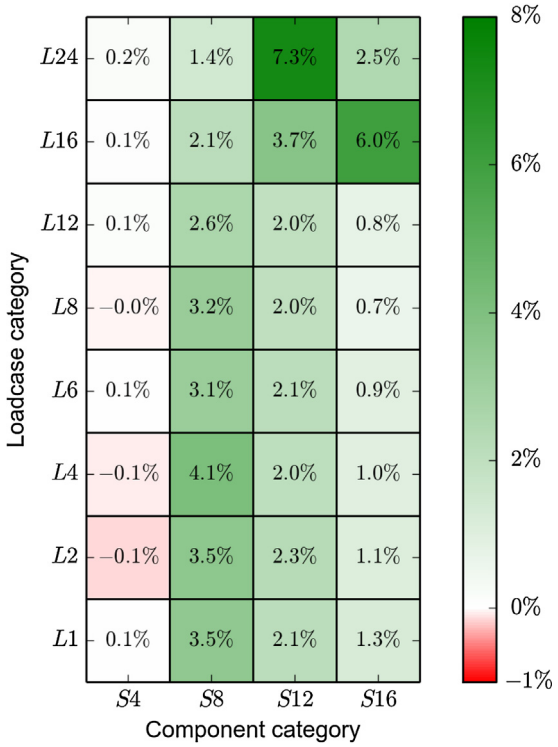

Fig. 7. Heatmap on the improvement of solution quality of AdaptDiscAlgo in relation to MINLP$^{\text{lin,feas}}$; averaged for each test instance category.

sizing: from 11.45 MW to 12.02 MW. By this change, the solution becomes feasible. The three approaches mentioned in Table 1 lead to three different DESS structures, whereby the solution of AdaptDiscAlgo has the best objective value, i.e., net present value. In fact, AdaptDiscAlgo's solution has, compared to the computed result of MINLP, a 28% higher net present value. With regard to MINLP$^{\text{lin,feas}}$, the presented AdaptDiscAlgo leads to a slightly, i.e., 3%, better solution. Looking at the DESS structures it turns out that using a second compressor chiller and a second absorption chiller is profitable in this problem instance. Furthermore, the total size of the boilers decrease, while the net present value of the three DESS systems increases.

In the further course of the computational results we evaluate the performance of AdaptDiscAlgo regarding objective value and computation times on the basis of the entire set of 320 problem instances. Among other things, we will see that the instance chosen for Table 1 is a good representative, in the sense that the solutions of AdaptDiscAlgo outperform the two benchmarking approaches.

For evaluating the quality of a feasible solution of a problem, we consider the *primal gap* to the objective value of a given reference solution, i.e., an optimal or other known solution.

Definition 1. The *primal gap* of a feasible solution x with objective value $f(x)$ and a reference solution $x^\star$ with objective value $f(x^\star)$ is, except for trivial cases, defined by $\text{gap}_p(x, x^\star) := \frac{f(x)-f(x^\star)}{|f(x^\star)|}$.

We compute averages over parts of the test instances using the *shifted geometric mean*, which is customary in computational optimization, see Achterberg (2007).

Definition 2. The *shifted geometric mean* of numbers $a_1, \ldots, a_k \in \mathbb{R}$ and a shift $\zeta \in \mathbb{R}_+$ with $(a_i + \zeta) > 0$, $i = 1, \ldots, k$ is defined by

$$\gamma_\zeta(a_1, \ldots, a_k) := \left(\prod_{i=1}^{k} (a_i + \zeta) \right)^{(1/k)} - \zeta. \tag{30}$$

We use a shift of $\zeta = 100$ for time in seconds and values in percent, e.g., primal-dual bound, and a shift of $\zeta = 10$ for number of iterations.

The computational results of the solution quality of the benchmark MINLP and AdaptDiscAlgo is represented by a heatmap in Fig. 6. For every test instance category, the average of relative improvement of the best solution of AdaptDiscAlgo in comparison to the best solution of MINLP (1)–(12) is indicated by the percentage and coloring of the heatmap square. To put it briefly, the greener, the better the solution quality of AdaptDiscAlgo compared to MINLP. The averages are calculated with the best MINLP solution as reference solution (Definition 1) and only instances are considered where both approaches provide an MINLP solution. Additionally and enclosed in brackets, the number of test instances (max. ten per category) is given, for which AdaptDiscAlgo (right number) respectively MINLP (left) computes an MINLP solution within the time limit.

For the smallest test instances, MINLP was able to solve every test instance of categories $S4L\{1, 2, 4, 6\}$ optimally within the time limit. For 63% (202 out of 320) of all considered test instances, at least a feasible solution was computed by MINLP, in all other cases the time limit was reached without any primal solution. In contrast, AdaptDiscAlgo was able to compute an MINLP feasible solution for every single test instance. Of course, the proposed algorithm cannot ensure optimality of its solutions. However, AdaptDiscAlgo provides near-optimal solutions for test instances solved optimally by MINLP. Irritatingly, in category *S4L6*, AdaptDiscAlgo computes on an average a 0.1%-better solution than an (according to BARON) globally *optimal* solution of MINLP. This is due to the fact that BARON cuts off optimal solutions during the solution process for some of these instances. Unfortunately, this is not unusual in computational (nonlinear) optimization due to limited machine accuracy. All in all, except for the smallest instance categories, AdaptDiscAlgo is able to compute up to 40% better MINLP solutions than MINLP.

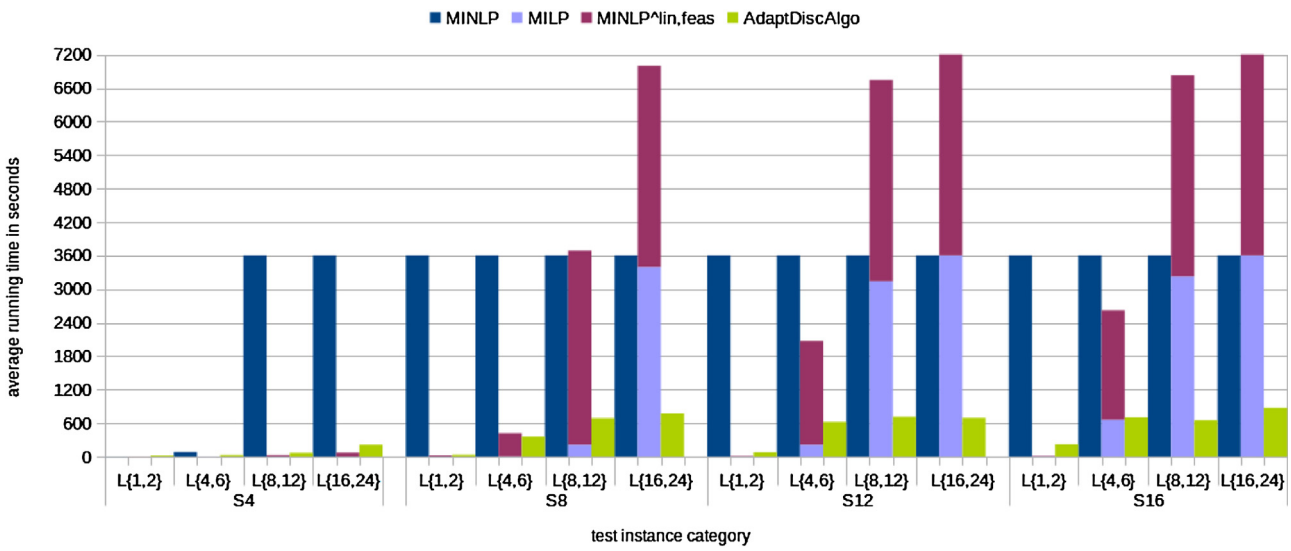

Fig. 8. Average running times of MINLP, MILP, MINLP^{lin,feas} and AdaptDiscAlgo.

All primal bounds, dual bounds and computation times of the MINLP and AdaptDiscAlgo of the computations executed for this work are online available at DESSLib (Bahl et al., 2016).

Since common DESS-solving approaches consist of piecewise linearized models (Section 1), we compare approximate solutions of such a model with MINLP solutions of the proposed AdaptDiscAlgo following the explanations in Section 2.3. The structure y_s^* and sizing decisions V_s^{N*} of MILP solutions are in 85%, i.e., 273 out of 320 test instances, not feasible in the original MINLP problem. If it was feasible, it was a test instance of small-sized category *S*4. For this reason, we consult MINLP^{lin,feas} (13)–(15) to compute a MINLP-feasible solution *close to* the approximate MILP solution and evaluate it with the original objective (1). The comparison of the solution quality of MINLP^{lin,feas} and AdaptDiscAlgo is shown by a heatmap in Fig. 7. The averages are calculated with MINLP^{lin,feas} solutions as reference solutions (Definition 1). In all categories, AdaptDiscAlgo provides comparably good or slightly better solutions as post-processed solutions of the piecewise-linearized approach.

The running times of all approaches are shown in Fig. 8. Since only instances of categories *S*4*L*{1, 2, 4, 6} are solved optimally by MINLP, for all other test instances, the running time reaches the limit of one hour. The piecewise linearized model (MILP) runs for most instances less than one hour. However, to obtain an MINLP-feasible solution through MINLP^{lin,feas}, this whole approach runs up to two hours. In comparison, the proposed AdaptDiscAlgo terminates generally after a fraction of an hour and thus outperforms the compared approaches in terms of solution quality as well as running time, except for the very smallest test instances.

The running time of AdaptDiscAlgo is split up over the parts of the algorithm as follows: on average 93% of the running time is used for solving the discretized MIP (Section 3.1) and 5 iteration steps are passed on an average until the stop criterion of convergence is satisfied. For all considered test instances, the feasibility NLP (Section 3.2) was feasible in every single iteration step. This was not the case for the alternative approaches of the discretized problem which are briefly mentioned in Section 3.4.

5. Summary and outlook

The superstructure-based synthesis of decentralized energy supply systems can be formulated as a mixed-integer nonlinear program. By including, e.g., nonlinear part-load performances, investment costs, and strict energy balances, this optimization problem is unavoidably nonconvex. In this paper, we do not circumvent this issue via approximating the problem by linearizing the performance and investment cost models of all considered types of equipment. Such approximate solutions from linearized problems are not necessarily feasible for the original nonlinear problem. In this paper, we set the focus on computing solutions which are feasible for the nonlinear synthesis problem. Since global MINLP solvers, e.g., BARON, have difficulties to provide primal solutions for real-world-based test instances, we propose a problem-specific solution approach for the nonlinear synthesis of DESS. This optimization-based algorithm consists of a discretized and linearly formulated version of the synthesis problem, whose underlying discretization grid is iteratively adapted. The resulting approximate problem is of such a nature that solution-specific decisions are also feasible in the original nonlinear problem and by solving a decomposable NLP, this leads to MINLP solutions. A computational study based on a set of test instances obtained from real industrial data shows that the proposed adaptive discretization algorithm computes better MINLP solutions in less computation times than state-of-the-art solvers. Thus, the proposed algorithm provides an efficient solution method to the synthesis of decentralized energy supply systems.

In future work, one should expand the adaptive discretization algorithm concerning methods to compute dual bounds for the MINLP to estimate the optimality gap of the algorithm's primal solutions. The (mostly very weak) dual bounds provided by BARON do not contribute meaningful information.

A mathematically feasible or even optimal solution is usually only an approximation of a real-world implementation, since a model never represents the real problem perfectly. Real world decisions might be influenced by constraints not represented in the model, e.g., (missing) maintenance knowledge in the company for specific technologies. In Voll et al. (2013a) and Hennen et al. (2016) we show that several near-optimal solution alternatives exist. Analyzing these near-optimal solutions allows to derive real-world decision options. Since the proposed AdaptDiscAlgo efficiently provides feasible solutions of the nonlinear synthesis problem, in future work the algorithm could be expanded to efficiently generate many near-optimal solution alternatives.

To identify the suitable superstructure, one could complement the proposed algorithm with the successive superstructure expansion method of Voll et al. (2013b).

The application of the proposed discretization algorithm to other hard to solve synthesis problems seems quite promising.

Appendix A. Economic parameters and equipment models

The economic parameters for the objective function, i.e., net present value, are taken from Voll et al. (2013b) and listed in Table A.2.

We list parameters of the considered types of equipment in A.3. Furthermore, we state the nonlinear models for part-load operation and investment cost curves used in this paper below. The part-load performance of CHP units is based on measured data-points for several existing units. Moreover, we assume that the part-load operation is not depending on the size of equipment, thus scaling to a normalized output power is possible. The part-load efficiency for boilers and absorption chillers is modeled in analogy to Fabrizio (2008). The part-load performance behavior is modeled in analogy to Fabrizio (2008) and additional correspondence with turbo compression manufacturers. The nominal efficiency of the CHP engines was taken from ASUE (2011). Maintenance-cost is based on IUTA (2002), the investment cost curves consider are composed on information from IUTA (2002) and databases of industrial partners.

Part-load performance: (A.1)–(A.5)

$s \in B$ (Boiler)

$$\dot{U}_s(\dot{V}_{s\ell}, \dot{V}_s^{\mathrm{N}}) = \frac{1}{\eta^{\mathrm{N,B}}} \left(C_1^{\mathrm{B}} \cdot \frac{\dot{V}_{s\ell}^2}{\dot{V}_s^{\mathrm{N}}} + C_2^{\mathrm{B}} \cdot \dot{V}_{s\ell} + C_3^{\mathrm{B}} \cdot \dot{V}_s^{\mathrm{N}} \right),$$
$$\eta^{\mathrm{N,B}} = 0.9, \quad C_1^{\mathrm{B}} = 0.1021, \quad C_2^{\mathrm{B}} = 0.8355, \quad C_3^{\mathrm{B}} = 0.0666 \tag{A.1}$$

$s \in A$ (Absorption chiller)

$$\dot{U}_s(\dot{V}_{s\ell}, \dot{V}_s^{\mathrm{N}}) = \frac{1}{\mathrm{COP}^{\mathrm{N,A}}} \left(C_1^{\mathrm{A}} \cdot \frac{\dot{V}_{s\ell}^2}{\dot{V}_s^{\mathrm{N}}} + C_2^{\mathrm{A}} \cdot \dot{V}_{s\ell} + C_3^{\mathrm{A}} \cdot \dot{V}_s^{\mathrm{N}} \right),$$
$$\mathrm{COP}^{\mathrm{N,A}} = 0.67, \quad C_1^{\mathrm{A}} = 0.8333, \quad C_2^{\mathrm{A}} = -0.0833, \quad C_3^{\mathrm{A}} = 0.25 \tag{A.2}$$

$s \in T$ (Turbo chiller)

$$\dot{U}_s(\dot{V}_{s\ell}, \dot{V}_s^{\mathrm{N}}) = \frac{1}{\mathrm{COP}^{\mathrm{N,T}}} \left(C_1^{\mathrm{T}} \cdot \frac{\dot{V}_{s\ell}^2}{\dot{V}_s^{\mathrm{N}}} + C_2^{\mathrm{T}} \cdot \dot{V}_{s\ell} + C_3^{\mathrm{T}} \cdot \dot{V}_s^{\mathrm{N}} \right),$$
$$\mathrm{COP}^{\mathrm{N,T}} = 5.54, \quad C_1^{\mathrm{T}} = 0.8119, \quad C_2^{\mathrm{T}} = -0.1688, \quad C_3^{\mathrm{T}} = 0.3392 \tag{A.3}$$

Table A.2
Economic parameters of DESS synthesis problem.

$p^{\mathrm{el,buy}}$	$p^{\mathrm{el,sell}}$	$p^{\mathrm{gas,buy}}$	i	γ^{CF}
0.16 ct/kWh	0.10 ct/kWh	0.06 ct/kWh	0.08	10 a

Table A.3
Size ranges, maintenance cost factors, and minimum part-load factors of considered types of equipment.

	$\dot{V}_s^{\mathrm{N,min}}$	$\dot{V}_s^{\mathrm{N,max}}$	m_s	α_s^{min}
Boiler $s \in B$	0.1 MW	14 MW	1.5	0.2
CHP engine $s \in C$	0.5 MW	3.2 MW	10	0.5
Absorption chiller $s \in A$	0.05 MW	6.5 MW	1	0.2
Turbo chiller $s \in T$	0.4 MW	10 MW	4	0.2

$s \in C$ (CHP engine)

$$\dot{U}_s(\dot{V}_{s\ell}, \dot{V}_s^{\mathrm{N}}) = C_1^{\mathrm{C}} + C_2^{\mathrm{C}} \cdot \frac{\dot{V}_{s\ell}}{\dot{V}_s^{\mathrm{N}}} + C_3^{\mathrm{C}} \cdot \dot{V}_s^{\mathrm{N}} + C_4^{\mathrm{C}} \cdot \left(\frac{\dot{V}_{s\ell}}{\dot{V}_s^{\mathrm{N}}} \right)^2 + C_5^{\mathrm{C}} \cdot \dot{V}_{s\ell} + C_6^{\mathrm{C}} \cdot \left(\dot{V}_s^{\mathrm{N}} \right)^2, \quad C_1^{\mathrm{C}} = 550.3, \quad C_2^{\mathrm{C}} = -1328,$$
$$C_3^{\mathrm{C}} = -0.4537, \quad C_4^{\mathrm{C}} = 668.3, \quad C_5^{\mathrm{C}} = 2.649, \quad C_6^{\mathrm{C}} = 9.571e-05 \tag{A.4}$$

$$\dot{V}_s^{\mathrm{el}}(\dot{V}_{s\ell}, \dot{V}_s^{\mathrm{N}}) = C_7^{\mathrm{C}} + C_8^{\mathrm{C}} \cdot \frac{\dot{V}_{s\ell}}{\dot{V}_s^{\mathrm{N}}} + C_9^{\mathrm{C}} \cdot \dot{V}_s^{\mathrm{N}} + C_{10}^{\mathrm{C}} \cdot \left(\frac{\dot{V}_{s\ell}}{\dot{V}_s^{\mathrm{N}}} \right)^2 + C_{11}^{\mathrm{C}} \cdot \dot{V}_{s\ell} + C_{12}^{\mathrm{C}} \cdot \left(\dot{V}_s^{\mathrm{N}} \right)^2, \quad C_7^{\mathrm{C}} = 518.8, \quad C_8^{\mathrm{C}} = -1203,$$
$$C_9^{\mathrm{C}} = -0.5361, \quad C_{10}^{\mathrm{C}} = 579.3, \quad C_{11}^{\mathrm{C}} = 1.464, \quad C_{12}^{\mathrm{C}} = 7.728e-05 \tag{A.5}$$

Investment cost: (A.6)–(A.9)

$s \in B$ (Boiler)

$$I(\dot{V}_s^{\mathrm{N}}) = 1.85484 \cdot \left[\left(11418.6 + 64.115 \cdot \dot{V}_s^{\mathrm{N}\ 0.7978} \right) \cdot 1.046 \cdot \left(1.0917 - 1.1921 \cdot 10^{-6} \cdot \dot{V}_s^{\mathrm{N}} \right) \right] \tag{A.6}$$

$s \in A$ (Absorption chiller)

$$I(\dot{V}_s^{\mathrm{N}}) = 0.50401 \cdot 17554,18 \cdot \dot{V}_s^{\mathrm{N}\ 0.4345} \tag{A.7}$$

$s \in T$ (Turbo chiller)

$$I(\dot{V}_s^{\mathrm{N}}) = 0.8102 \cdot \dot{V}_s^{\mathrm{N}} \cdot \left(179.63 + 4991.3436 \cdot \dot{V}_s^{\mathrm{N}\ -0.6794} \right) \tag{A.8}$$

$s \in C$ (CHP engine)

$$I(\dot{V}_s^{\mathrm{N}}) = 9332.6 \cdot \left(\dot{V}_s^{\mathrm{N}} \cdot \frac{\eta_s^{\mathrm{N,el}}(\dot{V}_s^{\mathrm{N}})}{\eta_s^{\mathrm{N,th}}(\dot{V}_s^{\mathrm{N}})} \right)^{0.539},$$
$$\eta_s^{\mathrm{N,th}}(\dot{V}_s^{\mathrm{N}}) = 0.498 - 3.55 \cdot 10^{-5} \cdot \dot{V}_s^{\mathrm{N}}, \quad \eta_s^{\mathrm{N,el}}(\dot{V}_s^{\mathrm{N}}) = \eta_s^{\mathrm{N}} - \eta_s^{\mathrm{N,th}}(\dot{V}_s^{\mathrm{N}}), \quad \eta_s^{\mathrm{N}} = 0.87 \tag{A.9}$$

References

Achterberg, T., 2007. Constraint Integer Programming (Ph.D. thesis). Technische Universität Berlin.

Arcuri, P., Florio, G., Fragiacomo, P., 2007. A mixed integer programming model for optimal design of trigeneration in a hospital complex. Energy 32, 1430–1447, http://dx.doi.org/10.1016/j.energy.2006.10.023.

ASUE,2011. BHKW-Kenndaten 2011. In: Datenblatt. Arbeitsgemeinschaft für sparsamen und umweltfreundlichen Energieverbrauch e.V.

Bahl, B., Goderbauer, S., Arnold, F., Voll, P., Bardow, A., Koster, A., Lübbecke, M., 2016. DESSLib – Benchmark Instances for Optimization of Decentralized Energy Supply Systems. http://www.math2.rwth-aachen.de/DESSLib (accessed 07.06.16).

Bruno, J., Fernandez, F., Castells, F., Grossmann, I., 1998. A rigorous MINLP model for the optimal synthesis and operation of utility plants. Chem. Eng. Res. Des. 76, 246–258, http://dx.doi.org/10.1205/026387698524901 http://www.sciencedirect.com/science/article/pii/S0263876298716430.

Chen, C.-L., Lin, C.-Y., 2011. A flexible structural and operational design of steam systems. Appl. Therm. Eng. 31, 2084–2093, http://dx.doi.org/10.1016/j.applthermaleng.2011.03.007 http://www.sciencedirect.com/science/article/pii/S1359431111001396.

Dimopoulos, G.G., Frangopoulos, C.A., 2008. Optimization of energy systems based on evolutionary and social metaphors. Energy 33, 171–179, http://dx.doi.org/10.1016/j.energy.2007.09.002 http://www.sciencedirect.com/science/article/pii/S0360544207001600.

Drumm, C., Busch, J., Dietrich, W., Eickmans, J., Jupke, A., 2013. STRUCTese® – energy efficiency management for the process industry. Chem. Eng. Process: Process Intensif. 67, 99–110, http://dx.doi.org/10.1016/j.cep.2012.09.009 http://www.sciencedirect.com/science/article/pii/S0255270112001845.

Fabrizio, E., 2008. Modelling of multi-energy systems in buildings (Ph.D. thesis). Politecnico di Turino and Institut National des Sciences Appliquées de Lyon.

Farkas, T., Rev, E., Lelkes, Z., 2005. Process flowsheet superstructures: structural multiplicity and redundancy. Comput. Chem. Eng. 29, 2198–2214, http://dx.doi.org/10.1016/j.compchemeng.2005.07.008.

Frangopoulos, C.A., Spakovsky, M.R.v., Sciubba, E., 2002. A brief review of methods for the design and synthesis optimization of energy systems. Int. J. Appl. Thermodyn. 5, 151–160.

GAMS Development Corporation, 2015. General Algebraic Modeling System. (GAMS) http://www.gams.com.

Geißler, B., Martin, A., Morsi, A., Schewe, L., 2011. Using piecewise linear functions for solving MINLPs. In: Mixed Integer Nonlinear Programming. Springer Science + Business Media, pp. 287–314, http://dx.doi.org/10.1007/978-1-4614-1927-3_10.

Gupte, A., Ahmed, S., Cheon, M.S., Dey, S., 2013. Solving mixed integer bilinear problems using MILP formulations. SIAM J. Optim. 23, 721–744, http://dx.doi.org/10.1137/110836183.

Hennen, M., Lampe, M., Voll, P., Bardow, A., 2016. How to explore and analyze the decision space in the synthesis of energy supply systems. In: Proceedings of ECOS 2016 – The 29th International Conference on Efficiency, Cost, Optimization, Simulation and Environmental Impact of Energy Systems.

IBM, 2015. IBM ILOG CPLEX Optimization Studio. http://www.ilog.com/products/cplex (accessed 07.12.15).

Iman, R.L., Campbell, J., Helton, J., 1981. An approach to sensitivity analysis of computer models. I – introduction, input, variable selection and preliminary variable assessment. J. Qual. Technol. 13, 174–183.

IUTA,2002. Preisatlas – Ableitung von Kostenfunktionen für Komponenten der rationellen Energienutzung. In: Abschlussbericht. Institut für Energie- und Umwelttechnik e.V.

Jennings, M., Fisk, D., Shah, N., 2014. Modelling and optimization of retrofitting residential energy systems at the urban scale. Energy 64, 220–233, http://dx.doi.org/10.1016/j.energy.2013.10.076 http://www.sciencedirect.com/science/article/pii/S0360544213009432.

Kolodziej, S., Castro, P.M., Grossmann, I.E., 2013. Global optimization of bilinear programs with a multiparametric disaggregation technique. J. Glob. Optim. 57, 1039–1063, http://dx.doi.org/10.1007/s10898-012-0022-1.

Leyffer, S., Sartenaer, A., Wanufelle, E., 2008. Branch-and-refine for mixed-integer nonconvex global optimization. Preprint ANL/MCS-P 1547-0908. Argonne National Laboratory, Mathematics and Computer Science Division.

Lozano, M.A., Ramos, J.C., Carvalho, M., Serra, L.M., 2009. Structure optimization of energy supply systems in tertiary sector buildings. Energy Build. 41, 1063–1075, http://dx.doi.org/10.1016/j.enbuild.2009.05.008 http://www.sciencedirect.com/science/article/pii/S037877880900111X.

Maréchal, F., Kalitventzeff, B., 2003. Targeting the integration of multi-period utility systems for site scale process integration. Appl. Therm. Eng. 23, 1763–1784, http://dx.doi.org/10.1016/S1359-4311(03)00142-X http://www.sciencedirect.com/science/article/pii/S135943110300142X.

Maréchal, F., Weber, C., Favrat, D., 2008. Multiobjective design and optimization of urban energy systems. In: Pistikopoulos, E.N., Georgiadis, M.C., Kikkinides, E.S., Dua, V. (Eds.), Energy Systems Engineering. Process Systems Engineering, vol. 5. Wiley-VCH, Weinheim, Germany.

Østergaard, P.A., 2009. Reviewing optimisation criteria for energy systems analyses of renewable energy integration. Energy 34, 1236–1245, http://dx.doi.org/10.1016/j.energy.2009.05.004 http://www.sciencedirect.com/science/article/pii/S0360544209001777.

Papalexandri, K.P., Pistikopoulos, E.N., Kalitventzeff, B., 1998. Modelling and optimization aspects in energy management and plant operation with variable energy demands – application to industrial problems. Comput. Chem. Eng. 22, 1319–1333, http://dx.doi.org/10.1016/S0098-1354(98)00016-7 http://www.sciencedirect.com/science/article/B6TFT-3WTNY92-J/2/c4619100d5e2c4581678da2f2b88e278.

Papoulias, S.A., Grossmann, I.E., 1983. A structural optimization approach in process synthesis – I: utility systems. Comput. Chem. Eng. 7, 695–706, http://dx.doi.org/10.1016/0098-1354(83)85022-4 http://www.sciencedirect.com/science/article/B6TFT-43PRJJC-20/2/d103399965d19f265da6d82a661cb8a9.

Pham, V., Laird, C., El-Halwagi, M., 2009. Convex hull discretization approach to the global optimization of pooling problems. Ind. Eng. Chem. Res. 48, 1973–1979, http://dx.doi.org/10.1021/ie8003573.

Prokopakis, G.J., Maroulis, Z.B., 1996. Real-time management and optimisation of industrial utilities systems. Comput. Chem. Eng. 20 (Suppl. 1), S623–S628, http://dx.doi.org/10.1016/0098-1354(96)00113-5 http://www.sciencedirect.com/science/article/pii/0098135496001135.

Stojiljkovic, M., Stojiljkovic, M., Blagojevic, B., 2014. Multi-objective combinatorial optimization of trigeneration plants based on metaheuristics. Energies 7, 8554–8581, http://dx.doi.org/10.3390/en7128554.

Tawarmalani, M., Sahinidis, N.V., 2005. A polyhedral branch-and-cut approach to global optimization. Math. Program. 103, 225–249, http://dx.doi.org/10.1007/s10107-005-0581-8.

Tong, C., Palazoglu, A., El-Farra, N.H., Yan, X., 2015. Energy demand management for process systems through production scheduling and control. AIChE J. 61, 3756–3769, http://dx.doi.org/10.1002/aic.15033.

Varbanov, P., Doyle, S., Smith, R., 2004. Modelling and optimization of utility systems. Chem. Eng. Res. Des. 82, 561–578, http://dx.doi.org/10.1205/026387604323142603 http://www.sciencedirect.com/science/article/pii/S0263876204725289.

Varbanov, P.S., Perry, S., Klemes, J.J., Smith, R., 2005. Synthesis of industrial utility systems: cost-effective de-carbonisation. Appl. Therm. Eng. 25, 985–1001, http://dx.doi.org/10.1016/j.applthermaleng.2004.06.023 http://www.sciencedirect.com/science/article/pii/S1359431104002303.

Voll, P., Hennen, M., Klaffke, C., Lampe, M., Bardow, A., 2013a. Exploring the near-optimal solution space for the synthesis of distributed energy supply systems. Chem. Eng. Trans. 35, 277–282, http://dx.doi.org/10.3303/CET1335046.

Voll, P., Klaffke, C., Hennen, M., Bardow, A., 2013b. Automated superstructure-based synthesis and optimization of distributed energy supply systems. Energy 50, 374–388, http://dx.doi.org/10.1016/j.energy.2012.10.045 http://www.sciencedirect.com/science/article/pii/S0360544212008079.

Voll, P., Lampe, M., Wrobel, G., Bardow, A., 2012. Superstructure-free synthesis and optimization of distributed industrial energy supply systems. Energy 45, 424–435, http://dx.doi.org/10.1016/j.energy.2012.01.041 http://www.sciencedirect.com/science/article/pii/S0360544212000461.

Yokoyama, R., Shinano, Y., Taniguchi, S., Ohkura, M., Wakui, T., 2015. Optimization of energy supply systems by MILP branch and bound method in consideration of hierarchical relationship between design and operation. Energy Convers. Manage. 92, 92–104, http://dx.doi.org/10.1016/j.enconman.2014.12.020 http://www.sciencedirect.com/science/article/pii/S0196890414010498.

Yue, D., You, F., 2014. Game-theoretic modeling and optimization of multi-echelon supply chain design and operation under Stackelberg game and market equilibrium. Comput. Chem. Eng. 71, 347–361, http://dx.doi.org/10.1016/j.compchemeng.2014.08.010.

Zhao, H., Rong, G., Feng, Y., 2015. Effective solution approach for integrated optimization models of refinery production and utility system. Ind. Eng. Chem. Res. 54, 9238–9250, http://dx.doi.org/10.1021/acs.iecr.5b00713.